Structural aspects of stretched emeraldine as determined by X-ray scattering

B. K. Annis* and E. D. Specht†
**Chemistry and †Metals and Ceramics Division, Oak Ridge National Laboratory, PO Box 2008, Oak Ridge, Tennessee 37831-6197, USA*

and N. Theophilou and A. G. MacDiarmid
Department of Chemistry, University of Pennsylvania, Philadelphia, Pennsylvania 19104-6323, USA
(Received 9 February 1990; revised 15 May 1990; accepted 17 May 1990)

Small angle X-ray scattering experiments on amorphous and partially crystalline samples of polyaniline stretched by two different methods indicate the development of quite different structural features in the size range 5–100 nm. A qualitative comparison of wide angle scattering data shows that both processing methods produce orientation at the molecular level. The two types of scattering experiments indicate that the stretching processes result in reduced crystallinity. Doping the stretched polymers with Cl^- was found to produce changes in both large and small scale structure.

(Keywords: emeraldine; small angle X-ray scattering; polyaniline; conducting polymers)

INTRODUCTION

Of current interest in the area of conducting polymers is the enhancement of conductivity produced by stretching the material. This approach has been applied with success to polypyrrole[1], poly(*p*-phenylene vinylene)[2], polyacetylene[3], and recently to polyaniline[4]. In general stretching a polymer can introduce a variety of morphological effects, and the possible influence of the morphology on the conductivity is an open question. For example, the conductivity becomes anisotropic upon stretching, and in the case of polyacetylene, electron micrographs[7] showed that a substantial increase in the alignment of fibrils in the films occurred. A qualitative explanation for the difference in the conductivity parallel and perpendicular to the stretch direction is that in the latter an additional interfibril transfer is involved. Conversely, no evidence for fibril formation or alignment which could be correlated with conductivity changes was found for poly(*p*-phenylene vinylene)[2]. Further understanding is unlikely without additional information on the structural effects caused by the stretching process and, as part of an effort to characterize such effects in polyaniline, X-ray scattering techniques have been employed, and the results are presented here.

One of the techniques is small angle X-ray scattering (SAXS) which has provided information on a variety of features in the size range 5–100 nm (ref. 8). The scattering arises from fluctuations in the electron density which are typically due to the presence of microvoids, fibrils, and crystallites. Because of the variety of sources of the scattering, supplementary measurements can help to identify the nature of the scattering elements. Consequently, wide angle X-ray scattering (WAXS) was used to provide an indication of orientation at the molecular level and to establish the presence of crystallites in some of the samples.

‡ A recent review of the subject for semi-crystalline polymers has been given by Peterlin[5] and the behaviour of a number of amorphous polymers has been discussed by Berger[6]

EXPERIMENTAL

The polyaniline powders and solutions have been obtained by the technique described previously[9,10]. A polymeric stretchable support ($5 \times 2 \times 0.01$ cm) such as polypropylene, polyethylene, polybutadiene or poly(tetrafluoroethylene) (Teflon) was clamped in a laboratory stretching device and a ~2% solution of polyaniline (emeraldine base) in *N*-methylpyrrolidinone (NMP) was poured onto the substrate. A heating infra-red lamp (250 W, General Electric) was placed ~20 cm from the substrate, and the solvent was evaporated at ~60°C over ~20 min until the semi-solid resulting mixture was just no longer 'tacky' to the touch. At this time, the temperature was raised to 70–90°C (technique A) and to 110–150°C (technique B), and stretching was commenced at a rate of ~1 cm min^{-1} to stretching ratios up to $\sim l/l_0 = 3.5$ (where l = final length and l_0 = initial length)[4].

Four different batches of emeraldine base were used to provide samples for the X-ray investigation. The supports were removed and measurements were made on stretched and unstretched samples prepared from each batch, and in two instances samples which were stretched and subsequently doped with Cl^- by immersion in 1M HCl were also examined.

The SAXS experiments were done with the Oak Ridge National Laboratory SAXS facility[11] which makes use of a rotating anode X-ray source (Cu Kα), pinhole

0032-3861/91/071160-07

collimation, and a two-dimensional position-sensitive detector. Various angular ranges are obtained by changing the sample-to-detector position, and for this study distances of 1, 2 and 5 m were used. The corresponding range in momentum transfer was ~ 0.04–$4\ nm^{-1}$. Absolute intensities were obtained by calibration with a polyethylene standard[12]. The WAXS results were also obtained with a Cu Kα rotating anode source and a goniometer which provided for step scanning a scintillation detector. Both types of observations used the same samples which were composed of stacks of 5–10 μm thick films.

RESULTS AND DISCUSSION

Unstretched bases

Diffuse small angle scattering from an amorphous, unoriented polymer containing no impurities indicates the presence of voids in the material. The nature of the voids can be characterized by the angular distribution which is related to the size and the integrated scattering which is related to the volume fraction. Guinier's law[13] provides a means of extracting size information. It applies to the case of a monodisperse system of scattering elements and is given by

$$I(k) = I(0)\exp(-(kR_g)^2/3) \quad (1)$$

where $I(k)$ is the cross-section per unit volume (in units of cm^{-1}), the momentum transfer magnitude is given by $k = (4\pi/\lambda)\sin\Theta$, λ is the wavelength of the incident radiation and 2Θ is the scattering angle. The electronic radius of gyration is R_g, and in the case of a spherical scatterer, the sphere radius is $R_s = \sqrt{5/3}R_g$. The slope of a plot of $\ln I(k)$ *versus* k^2 provides a value for R_g. Generally, at larger angles, some degree of curvature is found in this type of plot and can be due to a distribution of sizes and deviations from sphericity.

The integral of the intensity over reciprocal space is related to the mean square fluctuation of the electron density and in the case of a two-phase, isotropic system this relationship may be written

$$Q = \int_0^\infty k^2 I(k)\,dk = 2\pi r_\tau^2(\rho_1 - \rho_2)^2\phi_1\phi_2 \quad (2)$$

the extension to three phases is given by[14]

$$Q = 2\pi_\tau^2\{(\rho_1 - \rho_2)^2\phi_1\phi_2 + (\rho_2 - \rho_3)^2\phi_2\phi_3 + (\rho_3 - \rho_1)^2\phi_3\phi_1\} \quad (3)$$

where Q is the so-called invariant, r_τ is the Thomson classical electron radius, and ρ_i and ϕ_i are the electron density and volume fraction, respectively, of the ith phase.

Some of the angular distribution data at the smallest angles for the samples designated AA and AC are plotted in the form of the Guinier equation in *Figure 1*. The corresponding values for the radii of gyration are tabulated in *Table 1*. For $k > 0.4\ nm^{-1}$ the scattered intensity for AC can be seen to be of greater magnitude than that for AA. This continued to be the case until $k = 2.5\ nm^{-1}$ and suggests a difference in the two samples. This was clarified by WAXS which found no evidence for crystallinity in AA whereas crystalline peaks are evident in the data for AC. Similar features have been noted previously by Moon *et al.*[15], Jozefowicz *et al.*[16], and Fosang *et al.*[17].

A complete interpretation of SAXS from a three-phase system (voids, amorphous, and crystalline) can be quite complicated[14,18]. However, the plot of a portion of the kernel of equation (2) as shown in *Figure 2* suggests that the contribution to the invariant from the crystalline and void phases are sufficiently well localized to permit an estimate of the volume fractions. A value of the invariant for the crystalline phase was obtained from the integral of the difference of $k^2I(k)$ for the partially crystalline and amorphous samples as shown in *Figure 2*. A density of $1.43\ g\ cm^{-3}$ was obtained from the unit cell of Moon *et al.*[15]. The density of the amorphous phase was determined to be $1.22\ g\ cm^{-3}$ by comparison with the densities of known liquids. Equation (2) was then used to provide an estimate of 0.03–0.05 for the volume fraction of the crystalline phase. If the entire invariant for sample AC was ascribed to the crystalline phase, a value of 0.08 would result. In the case of sample AA, application of

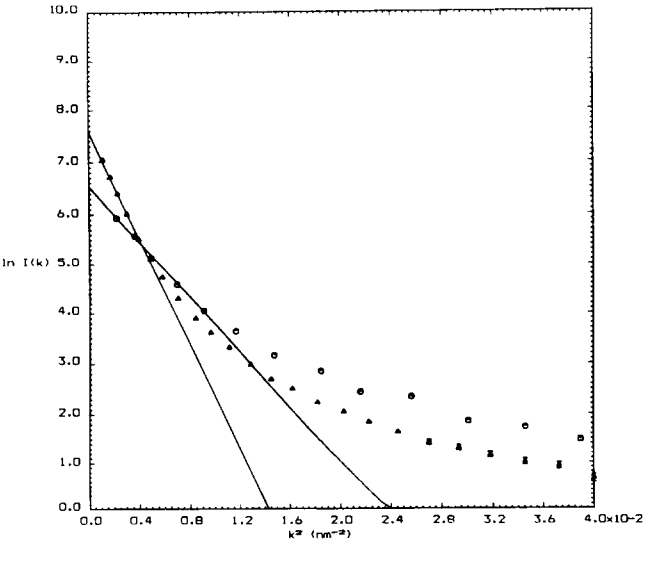

Figure 1 Guinier plots: ▲, sample AA, $R_g = 39$ nm; ○, sample AC, $R_g = 29$ nm. SAXS apparatus in 5 m configuration

Table 1 Data for the samples studied

Sample	R_g (nm)	Void fraction ($\times 10^{-4}$)	Crystalline fraction		L (nm)	W (nm)
			SAXS	WAXS		
AA	39	5				
AC	29	6	0.03–0.05	0.05	7.5 ± 2.5	8 ± 2
BA	32	3				
BC	28	4	0.02–0.03	0.05	6.0 ± 1.5	11 ± 2

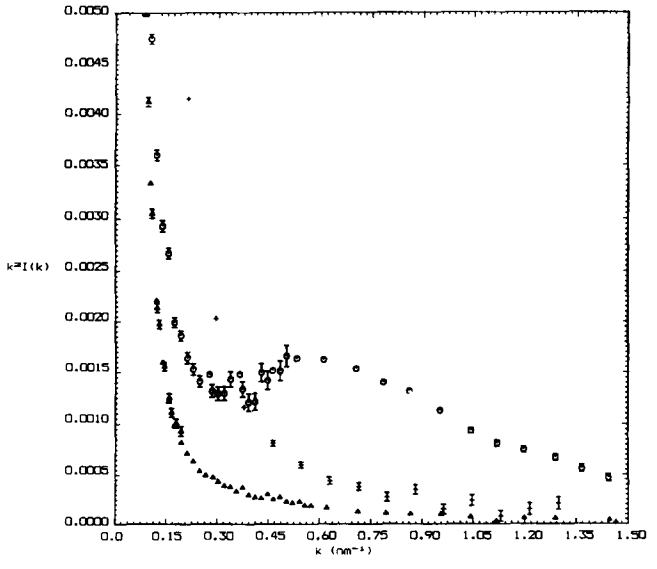

Figure 2 $I(k)k^2$ *versus* k: ▲, sample AA; ○, sample AC; a background of 0.018 (cm^{-1}) has been subtracted from each curve. +, The azimuthal average of the data for the 250% stretched sample corresponding to AC

equation (2) provides a value of 5×10^{-4} for the volume fraction of voids. For sample AC, extrapolation of the curve from $k = 0.2\ nm^{-1}$ outward with the 'Porod tail' model[19] results in a value of 6×10^{-4} for the volume fraction of voids. These values are quite similar to those obtained by Russell[20] on samples of Kapton by SAXS.

An estimate of the size of the crystallites can be obtained from the Porod 'distance of heterogeneity'[21]

$$L = \pi \int_0^\infty kI(k)\,dk/Q \qquad (4)$$

for spherical scatterers, the diameter of the sphere is given by $D = 4/3L$. The value of the integral in the numerator is more sensitive to the details of the calculation than is the case for the invariant integral, nevertheless, a value of 7.5 ± 2.5 nm results. A similar estimate of the crystallite size can be obtained from the WAXS data with the aid of the Scherrer formula

$$W = (0.88\lambda/\Delta(2\Theta)\cos\Theta) \qquad (5)$$

where $\Delta(2\Theta)$ is a full peak width at half maximum and W is an average dimension for roughly equiaxed objects (cf. ref. 22). From this approach, an average value of 8 ± 2 nm was obtained from the three peaks shown in *Figure 3*. An estimate of the crystallinity can also be made from the WAXS data, but unlike the SAXS estimate, it is quite sensitive to the choice of an amorphous background which must be subtracted. One approach is to simply draw a smooth curve across the base of the peaks, and this leads to a crystallite fraction of about 0.09. Another approach is to subtract an appropriately normalized amorphous curve. This would give a value of 0.01 but is quite sensitive to small errors in the normalization. The average value of 0.05 is in satisfactory agreement with the SAXS estimate.

Both SAXS and WAXS data for an amorphous and a partially crystalline sample from batches which were stretched by technique B were also obtained. The WAXS results from the amorphous sample are shown in *Figure 4*, and the data for the partially crystalline sample are analogous to that shown in *Figure 3*. A portion of the SAXS data are shown in *Figure 5*. There is a distinct

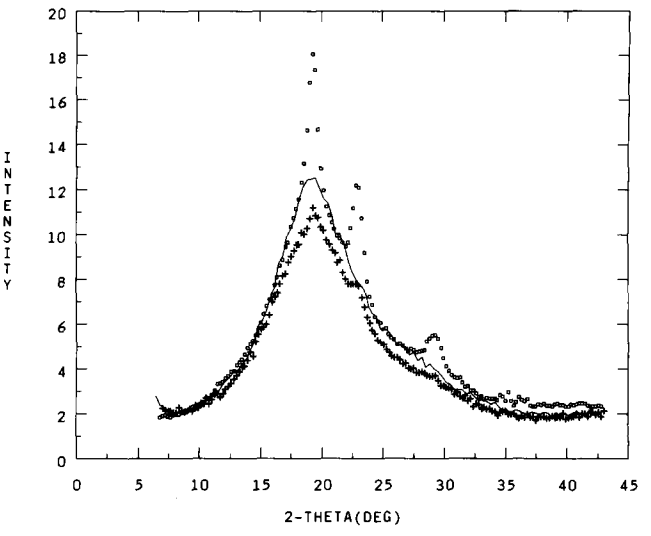

Figure 3 WAXS data from 250% stretched and unstretched versions of sample AC. ———, Axis vertical; +, axis horizontal; □, unstretched

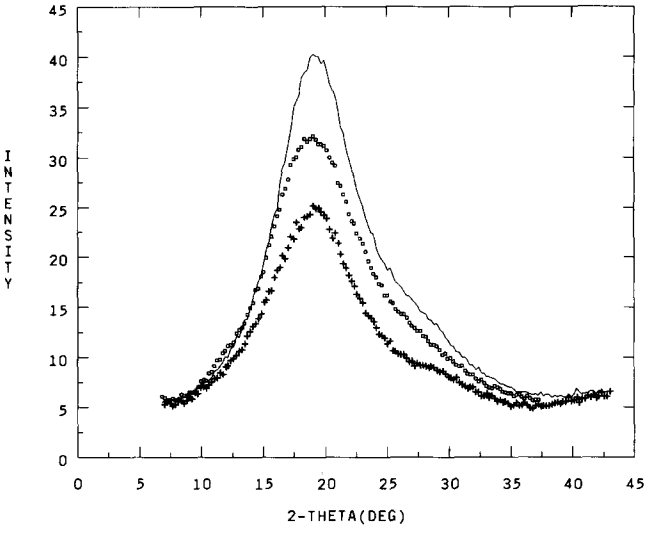

Figure 4 WAXS data from sample BA and the 350% stretched version of it. Intensities normalized by sample thickness. Symbols as in *Figure 3*

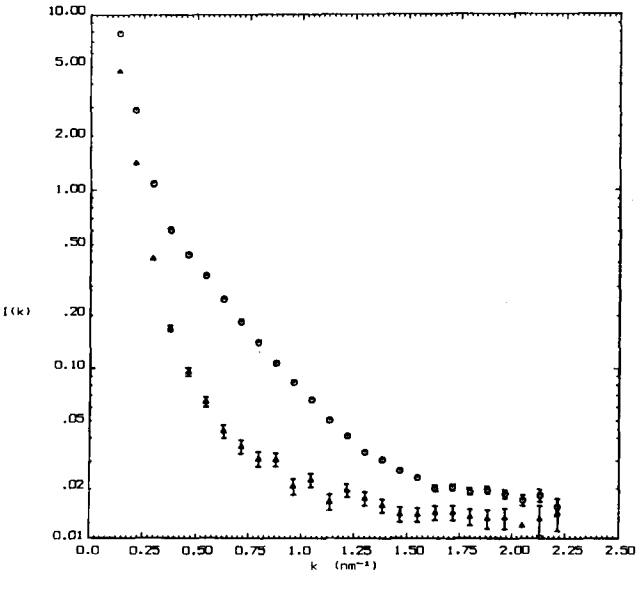

Figure 5 SAXS data with instrument in 2 m configuration: ○, unstretched sample BC; Δ, radial average of data from 250% stretched version

change in slope at $k \simeq 0.4\ nm^{-1}$ and a plot of Ik^2 *versus* k gives a result similar to that discussed for *Figure 2*. Analysis of the data as described above led to results which are summarized in *Table 1*.

Stretched bases

Contour plots of the scattering from two samples stretched by technique B are shown in *Figure 6*. The data was obtained with the SAXS apparatus in a configuration (5 m) that viewed the smallest scattering angles ($k \sim 0.04$–$0.4\ nm^{-1}$). *Figure 6a* is for a sample (designated BCS) which was stretched 250% and came from a partially crystalline batch. The corresponding unstretched sample has been designated BC. No anisotropy is evident, nor is there any indication of interference peaks which would indicate the presence of aligned scattering elements such as fibrils or lamellae. Such features with characteristic dimensions greater than 100 nm could exist but would not be observable. A comparison of the scattered intensity at larger angles for the stretched (BCS) and unstretched samples (BC) is shown in *Figure 5*. It is clear that the contribution ($k = 0.4$–$2.0\ nm^{-1}$) that was attributed to crystallites has disappeared in the processing. This reduction in crystallinity was confirmed by the WAXS data which was similar to that shown in *Figure 3*. Calculation of the invariant for the stretched sample gives a value less than half that attributed to voids in the unstretched sample, BC. The R_g value was determined to be 29 nm which is the same as that for BC within the experimental uncertainty. In essence, at the length scale accessible to the SAXS technique, the processing has tended to homogenize the material. However, WAXS results analogous to those shown in *Figure 3* indicate that this is not the case at the molecular level. A difference between the scans taken with the stretch axis coplanar (meridional) and perpendicular (equatorial) to the plane of the scan is typical of an oriented material. It should be noted that other X-ray[23] and spectroscopic[24] studies on other stretched emeraldine samples have been recently reported which provide a more quantitative measure of chain alignment.

Figure 6b was obtained from a sample that was stretched 350% (designated BAS) and which showed no indication of crystallinity in either the stretched or unstretched forms. The elongation of the contours perpendicular to the stretch direction is a common characteristic of SAXS from stretched polymers[25]. Due to the reciprocal nature of scattering, such a pattern indicates the presence of scattering elements with a minor axis perpendicular to the stretch axis. The eccentricity of the contour lines is quite small and amounts to only 1.1–1.2. Intensity profiles parallel and perpendicular to the stretch axis do not indicate any interference effects and are typical of diffuse polydisperse scatterers. This sample differs from that previously discussed (BCS) in that R_g is 25% larger than that of the corresponding unstretched sample, BA. This increase is accompanied by an increase of 30–50% in the invariant and is qualitatively consistent with a picture of relatively large voids which have expanded in a slightly anisotropic manner. SAXS data extending to $k = 4.5\ nm^{-1}$ were also obtained and showed no significant difference between the stretched and unstretched samples. WAXS data are shown in *Figure 4* and confirm that the processing has introduced anisotropy at the molecular level.

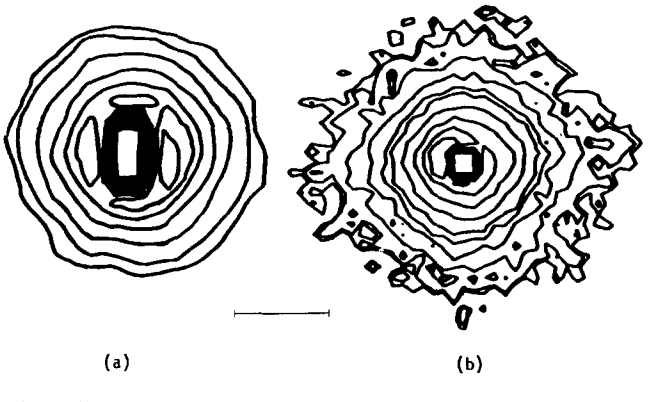

Figure 6 SAXS data with instrument in 5 m configuration: (a) 250% stretched version of sample BC; (b) 350% stretched version of sample BA. The outermost contours correspond to the same values of the scattered intensity and increase inward at the same rate. Stretch axis is vertical. (All contour plots have been corrected for background, detector response, absorption and put on an absolute intensity scale.) The line segment corresponds to $k = 0.1\ nm^{-1}$

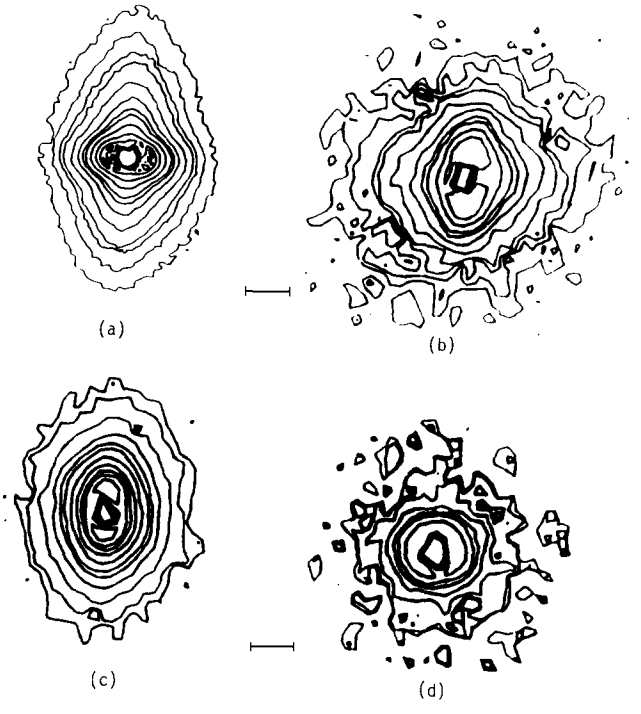

Figure 7 SAXS data for two stretched samples: (a) and (c) correspond to the stretched version of AA; (b) and (d) correspond to stretched version of AC. Stretch axis is vertical. (a) and (b) 5 m configuration; (c) and (d) 1 m configuration. The intensity contours for (a) are a factor of 10 greater than in (b). Those for (c) and (d) have the same value. The innermost contours for 1 m have the same value as the outermost at 5 m. The line segments correspond to $k = 0.1\ nm^{-1}$ for 5 m and $0.5\ nm^{-1}$ for 1 m

The isointensity contour plots for two samples stretched by technique A are shown in *Figure 7* and are substantially different from those discussed above. *Figure 7a* corresponds to the stretched version (300%) of the amorphous sample AA. The innermost contours are indicative of scattering elements elongated parallel to the stretch axis. However, as the angle increases, the scattering becomes dominated by elements which are elongated perpendicular to the stretch axis. Plots of slices of the intensity distributions in the two directions are shown in *Figure 8*. The slice parallel to the axis shows no evidence of any correlation effects, but a weak

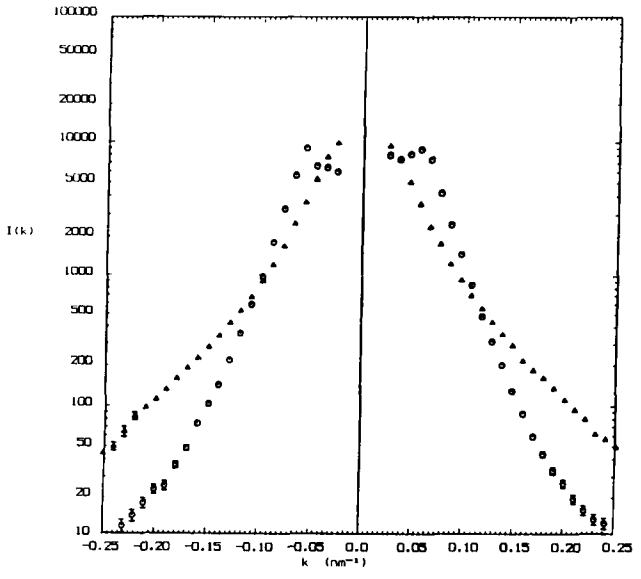

Figure 8 SAXS data from 300% stretched version of AA: ○, slice perpendicular to the stretch direction; ▲, slice parallel to the stretch axis

interference peak along the perpendicular direction is apparent.

If the scattering elements responsible for the peak are assumed to be aligned crystalline regions, then a consideration of the magnitude of the invariant requires that the volume fraction of such regions be about 0.03. By comparison with the results on samples AC and BC, it would be expected that WAXS should show evidence of crystalline peaks. However, the WAXS data proved to be quite similar to that shown in the data of *Figure 4*, and this suggests that the SAXS result is due to aligned amorphous fibrils. The Bragg law can be used to give an estimate[26] of the separation between the fibrils of 100 nm. Scanning electron microscopy (SEM) work[27] has indicated the presence of highly entangled fibrils on the surface of unstretched, doped polyaniline, and a scanning tunnelling microscopy study[28] also on unstretched, doped samples found regions on the surface which resembled partially aligned fibrils with separations of 100–200 nm. The SEM results[3,7] for stretched polyacetylene gave evidence for aligned, closely packed fibrils with a separation of 20 nm.

The general appearance of the contours of *Figure 7a* (sample AAS) is similar to SAXS results obtained in studies of crazing in polymers[29]. The crazes are envisioned to be microcracks or separations which developed perpendicular to a stress axis. The volume of the region of separation can be partially filled by fibrils with some degree of alignment parallel to the stress direction. However, the SAXS observations alone are insufficient to establish that this type of correlation between fibrils and voids was present in this sample. The volume fraction of voids was found to have increased by a factor of 15–20 in comparison with the unstretched sample AA and amounted to about 0.01. Most of this is due to voids oriented perpendicular to the stretch direction. The eccentricity of the contours outside the fibril region is 1.5–1.6, and a simple elongation of an existing void by this factor would not account for the increase in the volume fraction. Consequently, it would appear that the processing has increased the number of voids.

Figure 7b shows the isointensity contours for the stretched (250%) (sample ACS) corresponding to the partially crystalline sample, AC. There is no indication of fibril interference, and the scattering at lowest angles is due to scattering elements oriented perpendicular to the stretch axis. The maximum eccentricity of about 1.8–2.0 is similar to that for sample AAS, but, as can be seen in *Figure 7b* this source of scattering predominates over a much more limited range of angles. Because of the relatively rapid change in the orientation of the principle axis of the contours, it is difficult to rigorously determine the size of the scattering elements. Application of the Guinier approach to slices of the intensity distributions parallel and perpendicular to the stretch axis amounts to averaging over much of the central core of *Figure 7b* and results in an estimate of the radii of gyration of 25 and 22 nm, respectively.

Some of the azimuthally averaged SAXS data are included in *Figure 2*. Comparison with data from the corresponding unstretched, partially crystalline sample (AC) indicates substantially less scattering in the region which was attributed to crystallite scattering in AC. This is confirmed by the WAXS data for the two samples shown in *Figure 3*. The portion of the invariant computed from the SAXS data below $k = 0.2\ \text{nm}^{-1}$ is approximately two times larger than the equivalent region for the unstretched sample and is felt to be due to voids. This increase in the void scattering is substantially less than that for the 300% stretched sample (AAS) but is five to six times larger than that for sample BCS which was stretched an equivalent amount (250%) at higher temperature.

The emeraldine salt version of polyaniline which is formed by doping the films in 1 M HCl is of interest because of the electrical conductivity. If the only result of a doping process is to cause changes at the atomic and molecular level, and if this occurs uniformly on a scale greater than about 5 nm, then the contours observed in the SAXS measurements should remain the same while

Table 2

Sample	Stretch ratio	Void fraction	⊥,	R_g (nm),	∥	Peak ratio[a]
ACS	2.5	1×10^{-3}	22		25	1.2
AAS	3.0	1×10^{-2}	–		33	1.2
BCS	2.5	2×10^{-4}		29		1.2
BAS	3.5	4×10^{-4}		40		1.8
ACS (doped)	2.5	5×10^{-4}		28		1.1
BAS (doped)	3.5	9×10^{-4}	35		28	2.0

[a]WAXS ratio of equatorial (axis vertical) to meridional (axis horizontal) peak heights

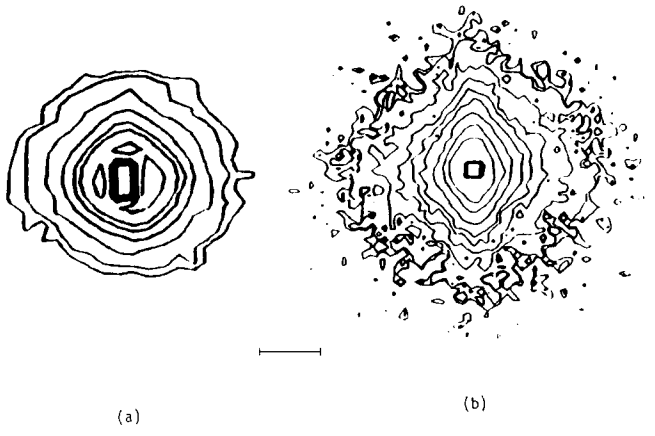

Figure 9 SAXS data from doped and stretched samples. Stretch axis was vertical, and instrument was in 5 m configuration: (a) corresponds to 250% stretched and doped version of AC; (b) corresponds to 350% stretched and doped version of BC. Outermost contours for both samples correspond to the same intensity. The line segment corresponds to $k = 0.1$ nm^{-1}

the intensities and invariants should change as the ratio of the square of the electron densities of the doped and undoped materials. The density of a number of doped samples which showed little if any indication of crystallinity by WAXS has been determined to be 1.34 ± 0.02 g cm^{-3}, and the corresponding ratio of the square of the electron densities is 1.18 ± 0.07. In the case of the unstretched material we have observed some differences between doped and undoped samples (primarily at the smallest observable angles) which exceed this ratio. As a preliminary effort in ascertaining the structural effects of doping, two of the stretched samples were doped with Cl^-. A comparison of *Figures 6b* and *9b* shows that the doped version of sample BA has developed scattering elements with an elongation perpendicular to the stretch axis. The R_g values perpendicular and parallel to the axis were found to be 35 and 28 nm, respectively, for the central region of the contour plot. This compares with a value of 40 nm found for the azimuthal average of the less anisotropic undoped sample. This feature accounts for most of the increase in the invariant which was found to be between two and two-and-a-half times larger than that for the undoped, stretched sample. At larger angles, the contours for both the doped and undoped samples indicate the presence of voids slightly elongated parallel to the stretch axis.

The SAXS isointensity contours for the doped version of the sample stretched 250% (ACS) with the low temperature process are shown in *Figure 9a*. Comparison with *Figure 7b* shows that the doping process tended to reduce the extent of large scale orientation. In addition, the invariant decreased to a value essentially the same as that attributed to the void contribution in the undoped, unstretched sample AC, and R_g for the azimuthally averaged intensity distribution was, within experimental uncertainty, the same as that for AC. While the doping seems to have had somewhat the opposite effect on the two samples, it is clear that changes are caused on a relatively large length scale. The WAXS results also indicate changes occurred at the molecular level. However, most of the change is similar to that observed in unstretched samples[15–17], the anisotropy as measured by the peak height ratio is changed relatively little. Further study of the doping effects is in progress.

CONCLUSIONS

The SAXS patterns from the emeraldine base films that were stretched at lower temperature (technique A) can be interpreted as arising from the presence of cracks or voids oriented perpendicular to the stretch axis. The quantity of voids increased with stretch ratio and was accompanied by an indication of interfibril interference. This implies the possibility of the onset of craze formation, i.e. the development of cracks containing fibrils. This is in qualitative accord with observations on a number of other glassy polymers at similar stretch ratios[5,6,29]. For films drawn at higher temperature, there was little indication of anisotropy on the scale of 5–100 nm, and no significant increase in the scattering due to the possible formation of bubbles, cracks or fibrils was found.

Neither the SAXS or WAXS observations provide evidence for an increase in crystallinity for stretch ratios of 3.5 or less. Instead, a reduction in crystallinity occurred using both techniques at a ratio of 2.5. Some degree of molecular orientation was found in the WAXS observations in all cases.

Doping the stretched films with Cl^- was found to affect the polymer on length scales observable by both SAXS and WAXS. However, the limited amount of data does not permit more specific conclusions to be made.

ACKNOWLEDGEMENTS

This research is sponsored by the Division of Materials Sciences, Office of Basic Energy Sciences, US Department of Energy under contract DE-AC05-84OR21400 with the Martin Marietta Energy Systems, Inc. Work at the University of Pennsylvania was supported in part by the Defense Advanced Research Projects Agency through a contract monitored by the Office of Naval Research and by NSF Grant No. DMR-86-15475. B. K. Annis is particularly grateful to the members of the ORNL Small Angle Scattering Center, J. S. Lin, S. Spooner and G. D. Wignall for their assistance and tutelage.

REFERENCES

1 Ogasawara, M., Funahashi, K., Demura, T., Hagiwara, T. and Iwata, K. *Synth. Met.* 1986, **14**, 61
2 Gagnon, D. R., Karasz, F. E., Thomas, E. L. and Lenz, R. W. *Synth. Met.* 1987, **20**, 85
3 Naarman, H. and Theophilou, N. *Synth. Met.* 1987, **22**, 1; European Patent EP 0295,430 (filed 13 May 1988)
4 Theophilou, N., MacDiarmid, A. G., Annis, B. K. and Epstein, A. J. March Meeting of the American Physical Society, 20–24 March 1989, St Louis, USA
5 Peterlin, A. *Colloid. Polym. Sci.* 1987, **265**, 357
6 Berger, L. L. *Macromolecules* 1989, **22**, 3162
7 Theophilou, N. and Naarman, H. 'Conducting Polymers' (Ed. L. Alcácer), D. Reidel Publishing Co., Netherlands, 1987, p. 65
8 Glatter, O. and Kratky, O. (Eds) 'Small Angle X-Ray Scattering', Academic Press, New York, 1982
9 MacDiarmid, A. G., Chiang, J. G., Richter, A. F., Somasiri, N. L. D. and Epstein, A. J. 'Conducting Polymers' (Ed. L. Alcácer), D. Reidel Publishing Co., Netherlands, 1987, p. 105
10 Angelopoulos, M., Asturias, G. E., Ermer, S. P., Ray, A., Scherr, E. M., MacDiarmid, A. G., Akhtar, M., Kiss, Z. and Epstein, A. J. *Mol. Cryst. Liq. Cryst.* 1988, **160**, 157
11 Wignall, G., Lin, J. S. and Spooner, S. *J. Appl. Crystal.* in press; Hendricks, R. W. *J. Appl. Cryst.* 1978, **11**, 15
12 Russell, T. P., Lin, J. S., Spooner, S. and Wignall, G. D. *J. Appl. Cryst.* 1988, **21**, 629
13 Alexander, L. E. 'X-Ray Diffraction Methods in Polymer Science', Wiley-Interscience, 1969, pp. 298–299

14 Goodisman, J. and Brumberger, H. *J. Appl. Cryst.* 1971, **4**, 347; Wu, W. *Polymer* 1982, **23**, 1907

15 Moon, Y. B., Cao, Y., Smith, P. and Heeger, A. J. *Polym. Commun.* 1989, **30**, 196

16 Jozefowics, M. E., Lavarsanne, R., Javadi, H. H. S., Epstein, A. J., Pouget, J. P., Tang, X. and MacDiarmid, A. G. *Phys. Rev. B, Rapid Commun.* 1989, **39**, 12958

17 Fosang, W., Jinsong, T., Lixiang, W., Hongfang, Z. and Zhishen, M. *Mol. Cryst. Liq. Cryst.* 1988, **160**, 175

18 Ciccariello, S. *Phys. Rev. B* 1989, **28**, 4301

19 Porod, G. *Kolloid-Z.* 1951, **124**, 83

20 Russell, T. P. *Polym. Eng. Sci.* 1984, **24**, 345

21 Guinier, A. and Fournet, G. 'Small-Angle Scattering of X-ray', John Wiley and Sons, 1955, p. 81

22 Schultz, J. M. 'Diffraction for Materials Scientists', Prentice-Hall, Inc., 1982, p. 226

23 Dyurado, D., Ma, J., Theophilou, N. and Fischer, J. E. *Synth. Met.* 1989, **30**, 395

24 Woo, H. S., Tanner, D. B., Theophilou, N. and MacDiarmid, A. G. *Bull. Am. Phys. Soc.* 1989, **34** (3), 823

25 Statton, W. O. 'Newer Methods of Polymer Characterization' (Ed. B. Ke), Interscience Publishers, 1964

26 Oster, G. and Riley, D. P. *Acta Cryst.* 1952, **5**, 272; Adams, W. W., Azároff, L. Y. and Kulshreshtha, A. K. *Z. Krist.* 1979, **150**, 321

27 Huang, W. S., Humphrey, B. D. and MacDiarmid, A. G. *J. Chem. Soc. Faraday Trans. 1* 1986, **82**, 2385; Chen, S. A. and Lee, T. S. *J. Polym. Sci., Polym. Lett. Edn* 1987, **25**, 455

28 Mantovani, J. G., Warmack, R. J., Annis, B. K., MacDiarmid, A. G. and Scherr, E. *J. Appl. Polym. Sci.* 1990, **40**, 1693

29 Garton, A., Stepaniak, R. F., Carlsson, D. J. and Wiles, D. M. *J. Polym. Sci., Polym. Phys. Edn* 1978, **16**, 599; Brown, H. R. and Kramer, E. J. *J. Macromol. Sci. Phys.* 1981, **B19**, 487; Dettenmaier, M. in 'Advances in Polymer Science 52/53, Crazing Polymers' (Ed. H. H. Kavsch), Springer-Verlag, Berlin, 1983, p. 57